Josephson currents in neutron stars

Armen Sedrakian
Institute for Theoretical Physics, Wrocław University
Frankfurt Institute for Advanced Studies

Scales 1st General Meeting, Jun 22-26, 2026
Physics Department, University of Coimbra

based on Phys. Rev. D 111, 023044 (2025) with Peter Rau

FIAS Frankfurt Institute for Advanced Studies

Uniwersytet Wrocławski

Pairing gaps and composition in the interior of a neutron star.

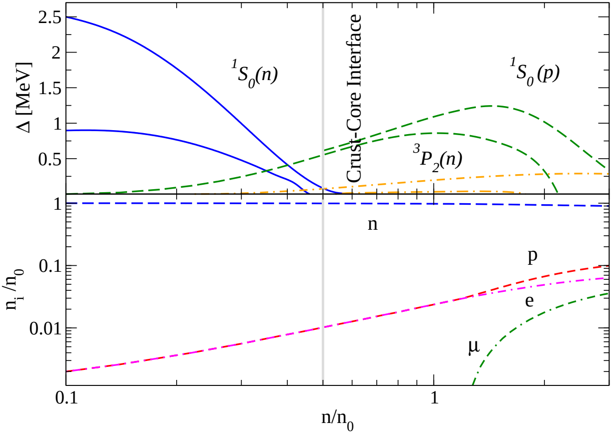

$^1S_0$ pairing of neutrons in the crust
$^3P_2$ pairing of neutrons in the core
$^1S_0$ pairing of protons in the core

In a two-fluid neutron–proton system, the mass currents are related to the transport velocities by the entrainment matrix as

$$\begin{pmatrix} \mathbf{j}_n \\ \mathbf{j}_p \end{pmatrix} = \begin{pmatrix} \rho_{nn} & \rho_{np} \\ \rho_{np} & \rho_{pp} \end{pmatrix} \begin{pmatrix} \mathbf{v}_n \\ \mathbf{v}_p \end{pmatrix}, \tag{1}$$

$\mathbf{j}_n, \mathbf{j}_p$ are the neutron and proton mass-current densities, $\mathbf{v}_n, \mathbf{v}_p$ are the neutron and proton superfluid velocities, ρ_{nn}, ρ_{pp} are the diagonal entrainment coefficients, ρ_{np} is the off-diagonal entrainment term. The diagonal and off-diagonal elements satisfy

$$\rho_{nn} + \rho_{np} = \rho_n, \qquad \rho_{pp} + \rho_{np} = \rho_p, \tag{2}$$

where ρ_n, ρ_p are the total neutron and proton mass densities.
The components of the matrix are given by

$$\rho_{nn} = \rho_n \frac{m}{m_n^*}, \quad \rho_{pp} = \rho_p \frac{m}{m_p^*}, \tag{3}$$

$$\rho_{np} = \rho_n \left(1 - \frac{m}{m_n^*}\right) = \rho_p \left(1 - \frac{m}{m_p^*}\right), \tag{4}$$

where m is the bare nucleon mass, and m_n^*, m_p^* are the neutron and proton effective masses.

Ginzburg-Landau functional for a superfluid-superconducting mixture in the core of the star

$$F = F_0 + F_{\rm kin} + F_{\rm cond} + F_{\rm em}, \qquad (5)$$

Condensate contribution (note static coupling between the condensates)

$$F_{\rm cond} = a_p |\psi_p|^2 + \frac{b_p}{2} |\psi_p|^4 + a_n |\psi_n|^2 + \frac{b_n}{2} |\psi_n|^4 + g_{np} |\psi_p|^2 |\psi_n|^2 . \qquad (6)$$

Kinetic energy contribution (note the entrainment)

$$F_{\rm kin} = \frac{1}{2}\rho_{pp} v_p^2 + \frac{1}{2}\rho_{nn} v_n^2 - \frac{1}{2}\rho_{pn} |\vec{v}_p - \vec{v}_n|^2 . \qquad (7)$$

The velocities are given by the phase gradient of the order parameter, plus the coupling to the vector potential for the protons,

$$\psi_j = |\psi_j| e^{i\theta_j} \qquad \boldsymbol{v}_j = \frac{\hbar}{2m_j}\left(\boldsymbol{\nabla}\theta_j - \frac{2e_j}{\hbar c}\boldsymbol{A}\right), \quad j = n, p, \qquad (8)$$

where $\hbar$ is the Planck constant, m_n/m_p is the mass of the neutron/proton, and θ_n/θ_p is the phase of the superfluid neutron/superconducting proton order parameter.

Minimization of the GL functional with respect to the order parameters yields the equations of motion

$$a_p\psi_p + b_p\left|\psi_p\right|^2\psi_p + g_{np}\left|\psi_n\right|^2\psi_p + \frac{1}{4m_p}\left(-i\hbar\boldsymbol{\nabla} - \frac{2e}{c}\boldsymbol{A}\right)^2\psi_p = 0, \tag{9}$$

$$a_n\psi_n + b_n\left|\psi_n\right|^2\psi_n + g_{np}\left|\psi_p\right|^2\psi_n - \frac{\hbar^2}{4m_n}\nabla^2\psi_n = 0, \tag{10}$$

with $a_{n,p} < 0$ (superfluid phase), $b_{n,p} > 0$. Here $\boldsymbol{A}$ is the vector potential, e the unit charge, g_{np} the inter-component coupling, and $m_{n/p}$ the bare masses.

The boundary condition at the interface generalizes the standard GL form to include pair tunneling

$$\boldsymbol{n}\cdot\left(\boldsymbol{\nabla} - \frac{2ie}{\hbar c}\boldsymbol{A}\right)\psi_{1,2,j}\Big|_{\text{Boundary}} = \pm\frac{\psi_{2,1,j}|_{\text{Boundary}}}{\zeta_j}, \tag{11}$$

where $j = n, p$, ζ_j^{-1} measures barrier transparency, and $\boldsymbol{n}$ is the unit normal to the boundary.

Josephson currents in neutron stars

A Sedrakian

Stationary Josephson effect at the S-P interface

Dynamical Josephson effect and energy radiation

Minimization of the GL functional with respect to the $\boldsymbol{A}$ and $\boldsymbol{v}_n$ gives the currents:

$$\boldsymbol{j}_p = \frac{e\hbar}{2m_p^2}\left(\rho_{pp}-\rho_{pn}\right)\left(\boldsymbol{\nabla}\theta_p - \frac{2e}{\hbar c}\boldsymbol{A}\right) + \frac{e\hbar}{2m_p m_n}\rho_{pn}\boldsymbol{\nabla}\theta_n, \tag{12}$$

$$\boldsymbol{j}_n = \frac{\hbar}{2m_n}\left(\rho_{nn}-\rho_{pn}\right)\boldsymbol{\nabla}\theta_n + \frac{\hbar}{2m_p}\rho_{pn}\left(\boldsymbol{\nabla}\theta_p - \frac{2e}{\hbar c}\boldsymbol{A}\right). \tag{13}$$

Unlike the ordinary currents in the GL theory, these expressions depend on the phase gradients of both order parameters, coupled through the entrainment parameter ρ_{np}. Eliminate the phase gradients $\boldsymbol{\nabla}\theta_{p/n}$ from the expressions for the currents

$$\left(\psi_j^*\boldsymbol{\nabla}\psi_j - \psi_j\boldsymbol{\nabla}\psi_j^*\right) = 2i\left|\psi_j\right|^2\boldsymbol{\nabla}\theta_j = i\frac{\rho_{jj}}{m_j}\boldsymbol{\nabla}\theta_j, \tag{14}$$

where we substituted $\psi_j = \left|\psi_j\right| e^{i\theta_j}, j = n, p$ and defined $2m_j\left|\psi_j\right|^2 = \rho_{jj}$.

The combination of the current equations with gauge invariance $\boldsymbol{A} \to \boldsymbol{A} + \boldsymbol{\nabla}\theta$ yields the Josephson currents across the interface

$$\boldsymbol{n} \cdot \boldsymbol{j}_p = \frac{e\hbar}{m_p \zeta_p} \frac{(\rho_{pp} - \rho_{pn})}{\rho_{pp}} |\psi_{1,p}| \, |\psi_{2,p}| \sin(\Delta\theta_p) + \frac{e\hbar}{m_p \zeta_n} \frac{\rho_{pn}}{\rho_{nn}} |\psi_{1,n}| \, |\psi_{2,n}| \sin(\Delta\theta_n) \,, \tag{15}$$

$$\boldsymbol{n} \cdot \boldsymbol{j}_n = \frac{\hbar}{\zeta_n} \frac{\rho_{nn} - \rho_{pn}}{\rho_{nn}} |\psi_{1,n}| \, |\psi_{2,n}| \sin(\Delta\theta_n) + \frac{\hbar}{\zeta_p} \frac{\rho_{pn}}{\rho_{pp}} |\psi_{1,p}| \, |\psi_{2,p}| \sin(\Delta\theta_p) \,. \tag{16}$$

The gauge-invariant phase difference

$$\Delta\theta_i = \theta_{2,i} - \theta_{1,i} - \frac{2\pi}{\Phi_0} \delta_{i,p} \int_{\mathcal{C}} \boldsymbol{A} \cdot d\boldsymbol{l}. \tag{17}$$

Here $\Phi_0 = \pi\hbar c/e$ is the proton flux quantum and δ_{ip} the Kronecker delta.

- Phase differences drive stationary supercurrents across the interface
- Neutron phase mismatch $\Delta\theta_n$ is the driver. Origin: ${}^1S_0 \to {}^3P_2$–${}^3F_2$ transition
- Entrainment converts neutron phase gradients to proton supercurrent $\to$ coupled neutron–proton Josephson transport

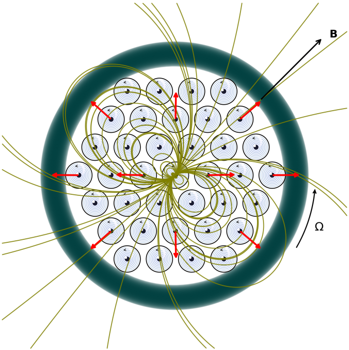

- On secular time scales, neutron vortices move outward and cross the interface

$$\frac{\partial N}{\partial t} + \mathrm{div}(N\boldsymbol{v}_L) = 0, \qquad v_{Lr} = -\frac{\dot{\Omega}}{2\Omega}r. \tag{18}$$

- **Assumption:** On long time scales, proton flux tubes, intertwined with neutron vortices, move with the same velocity v_{Lr} determined by the secular evolution.

- The outward motion of neutron vortex lines serves as a source of time-dependent Josephson currents across the interface:

$$\boldsymbol{v}_n = \frac{\hbar}{2m_n}\boldsymbol{\nabla}\theta_n = \frac{n\hbar}{2m_n\varrho}\hat{\varphi}. \tag{19}$$

- Neutron vortex is moving through the interface → neutron order parameter has a time-dependent phase

$$\Delta\theta_n = \theta_{1,n} - \theta_{2,n} + \omega_V t, \tag{20}$$

where $\theta_{1,n}$ and $\theta_{2,n}$ are the static phases; $\omega_V t$ is a time-dependent part induced by the motion.

- The period $2\pi/\omega_V$ is given simply by

$$\omega_V = \frac{v_{Lr}}{d_n}. \tag{21}$$

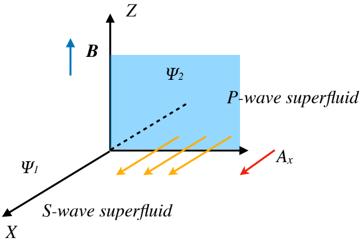

- Entrainment implies that time-dependent neutron phase induces a *time-dependent proton current* through the junction given by

$$j_V \equiv \boldsymbol{n} \cdot \boldsymbol{j}_p(t) = j_{0,pn} \sin\left(\theta_{2,n} - \theta_{1,n} + \omega_V t\right), \tag{22}$$

$$j_{0,pn} \equiv \frac{e\hbar}{m_p \zeta_n} \frac{\rho_{pn}}{\rho_{pp}} |\psi_{1,n}||\psi_{2,n}|. \tag{23}$$

- The time-dependent dipole, and therefore the associated current, radiates an electromagnetic wave. The time-averaged radiated power is

$$\langle P \rangle = \frac{2\langle \dot{I}^2 \rangle d^2}{3c^3}, \tag{24}$$

where I is the current and d the characteristic length scale.

- For a single vortex crossing the interface, the current is $I = j_V(\ell_\perp \ell_z)$, giving

$$\langle P_V \rangle = \frac{(j_{0,pn}\omega_V)^2}{3c^3}(d\ell_\perp \ell_z)^2. \tag{25}$$

where $\ell_{\perp,z}$ are the transverse and parallel extensions of the vortex in a spherical container (star).

Summing over vortices, with vortex density on the equator $N_V = 2\pi R/d_n$ and assuming (approximate) cylindrical geometry yields

$$\langle \mathcal{P}_{\star,V} \rangle = 3 \times 10^7 \; \tau_5^{-2} \; R_6^5 \; \Omega_{100}^{3/2} \; \text{erg s}^{-1}. \tag{26}$$

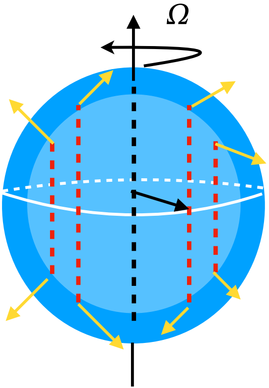

This is negligible compared to standard heating mechanisms such as Ohmic dissipation,

$$\mathcal{P}_{\text{Ohm}} \sim 10^{27} \; \text{erg s}^{-1}. \tag{27}$$

- Each neutron vortex carries on average 10^{13} proton flux-tubes $\rightarrow$ the frequency of the oscillations due to flux-tube motion is much higher. The intervortex distances for vortices and flux-tubes follow from rotation frequency and magnetic field for NS are

$$d_n \simeq 10^{-3} \text{ cm}, \quad d_p \simeq 10^{-10} \text{ cm}; \tag{28}$$

- The passage of a flux tube induces a *time-dependent flux* in the junction,

$$\omega_p = \frac{v_{Lr}}{d_p}, \qquad \Phi_*(t) = \Phi_{\max} \cos(\omega_p t), \tag{29}$$

leading to an oscillating Josephson current

$$j_\Phi = j_{0,pp} \sin\left[\Delta\theta_p + \frac{\Phi(t)}{\Phi_0}\right]. \tag{30}$$

- The corresponding radiated power is

$$\langle P_\Phi \rangle = \frac{(j_0\omega_p)^2}{6c^3}(d\ell_\perp \ell_z)^2. \tag{31}$$

Computation of the radiation from the entire star gives:

$$\langle P_{\star,V}\rangle = \frac{\alpha_e\pi\eta_n^2}{6}\left(\frac{v_{Fn}}{c}\right)^2\left(n_n\lambda^2R\right)^2\left(\frac{R}{d_n}\right)^3\frac{\hbar}{\tau^2}, \quad \text{(vortex)} \qquad (32)$$

$$\langle P_{\star,\Phi}\rangle = \frac{\alpha_e\pi\eta_p^2}{12}\left(\frac{v_{Fp}}{c}\right)^2\left(n_p\lambda^2R\right)^2\left(\frac{R}{d_p}\right)^3\frac{\hbar}{\tau^2}, \quad \text{(flux-tube)} \qquad (33)$$

where $\eta_p \equiv (1-\kappa_{np})/(2\zeta_p k_{Fp})$ and the pulsar lifetime is defined as $\tau^{-1} = |\dot{\Omega}|/\Omega$. The final result for the flux tubes is

$$\langle P_{\star,\Phi}\rangle = 2\times 10^{28}\,\tau_5^{-2}R_6^5\,B_{13}^{3/2}\ \text{erg s}^{-1}. \qquad (34)$$

This can be compared to Ohmic dissipation:

$$\mathcal{P}_{\rm Ohm} \simeq 10^{27}\left(\frac{B_{\rm cr}}{10^{13}\ \rm G}\right)^2\left(\frac{10^{23}\ \rm s^{-1}}{\sigma}\right)\left(\frac{\delta R}{0.5\ \rm km}\right)\text{erg s}^{-1}. \qquad (35)$$

Stationary case:

- The interface between S-wave and P-wave superfluids acts as a Josephson junction, generating supercurrents driven by phase differences.
- A stationary neutron current across the interface, entrains protons and induces a co-moving proton current, which exhibits Josephson oscillations.

Time-dependent case:

- The secular deceleration of a neutron star reduces the density of neutron vortices via their outward motion from the rotation axis towards the boundary surface.
- This motion of neutron vortices induces a similar motion of proton flux tubes and produces time-dependent Josephson currents, with frequencies set by vortex velocity and flux-tube spacing.

Phenomenological implications:

- The oscillating Josephson currents generate electromagnetic radiation, leading to heating of the neutron star interior.
- The heating rate is temperature-independent, but depends on spin frequency, its derivative, and the magnetic field strength.
- The mechanism operates on secular timescales and is not suited for transient phenomena such as glitches.

Josephson currents in neutron stars

A Sedrakian

Stationary Josephson effect at the S-P interface

Dynamical Josephson effect and energy radiation

– Direct experimental realisation of the physics discussed in the preceding sections is provided by the atomtronic Josephson junction necklace (JJN) of Pezzè, Xhani et al. (2024) "Stabilizing persistent currents in an atomtronic Josephson junction necklace"

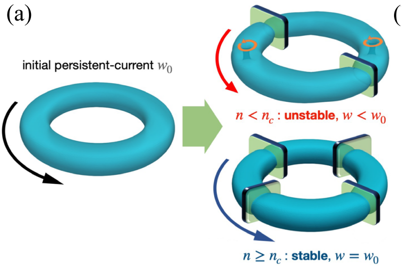

Fig. 3 | Sketch of the experiment and observables. a After preparing an initial persistent current state with circulation w_0, the n junctions are ramped up (see text). The 3D density plots are isosurfaces obtained from 3D GPE numerical simulations of the experimental set-up. If n is below a critical value n_c depending o w_0, the initial current is dissipated via the nucleation of vortices (here $n = 2$ and vortices are highlighted by orange cycling arrows in the upper right plot). Conversely, if $n \geq n_c$ (here $n = 4$), the system remains stable with $w = w_0$ (lower right

–A molecular Bose-Einstein condensate (BEC) of ^{6}Li dimers is confined in a ring-shaped trap of mean radius.

– Persistent current states with quantized winding number w

– The critical winding number $w_c(n)$ the current decays grows monotonically with n.

Gross-Pitaevskii model of two coupled Bose condensates

From time-dependent variational principle $i\hbar\,\partial_t\Psi_j = \delta E/\delta\Psi_j^*$:

$$i\hbar\frac{\partial\Psi_1}{\partial t} = -\frac{\hbar^2}{2m_1^*}\left(\boldsymbol{\nabla} - \frac{iq}{\hbar c}\boldsymbol{A}\right)^2\Psi_1 + \frac{\hbar^2\rho_{12}}{2m_1m_2}\boldsymbol{\nabla}^2\Psi_2\,\frac{\Psi_1}{|\Psi_1|} + \left(g_{11}|\Psi_1|^2 + g_{12}|\Psi_2|^2\right)\Psi_1,$$

Varying E with respect to Ψ_2^* yields the GP equation for the passive condensate,

$$i\hbar\frac{\partial\Psi_2}{\partial t} = -\frac{\hbar^2}{2m_2^*}\boldsymbol{\nabla}^2\Psi_2 + \frac{\hbar^2\rho_{12}}{2m_1m_2}\left(\boldsymbol{\nabla} - \frac{iq}{\hbar c}\boldsymbol{A}\right)^2\Psi_1\,\frac{\Psi_2}{|\Psi_2|} + \left(g_{22}|\Psi_2|^2 + g_{12}|\Psi_1|^2\right)\Psi_2,$$

– When $\rho_{12} = 0$ both equations decouple into standard single-species GP equations, with effective masses $m_j^* = m_j^2/\rho_{jj}$ modifying the kinetic terms.
– The cross terms $\propto \rho_{12}$ encode the non-dissipative drag (entrainment) between the two condensates.

–The gauge field $\boldsymbol{A}$ enters the equation of motion for the passive condensate 2 through the entrainment term: even though condensate 2 carries no charge, it is subject to the gauge field indirectly via its coupling to condensate 1.

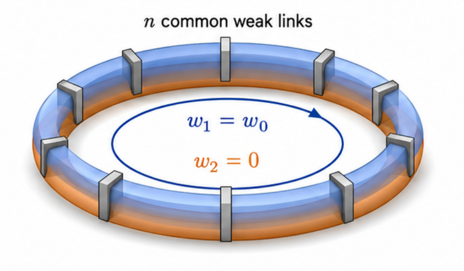

Extension would be to load a *second hyperfine state* of ^{6}Li simultaneously into the same ring trap, creating a two-component BEC. The two spin states interact via the interspecies contact coupling $g_{12} = 2\pi\hbar^2 a_{12}/m_{12}$, which is tunable over a wide range via Feshbach resonances.

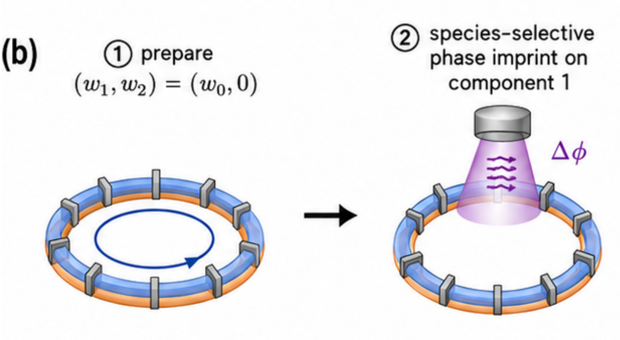

Active condensate 1: the spin state that is phase-imprinted and carries the initial winding number w. It couples to the rotating-frame vector potential $\boldsymbol{A}_{\rm rot}$

Passive condensate 2: the second spin state, initially prepared with $w_2 = 0$ (no imprinted circulation). It carries no phase winding and hence no net angular momentum.

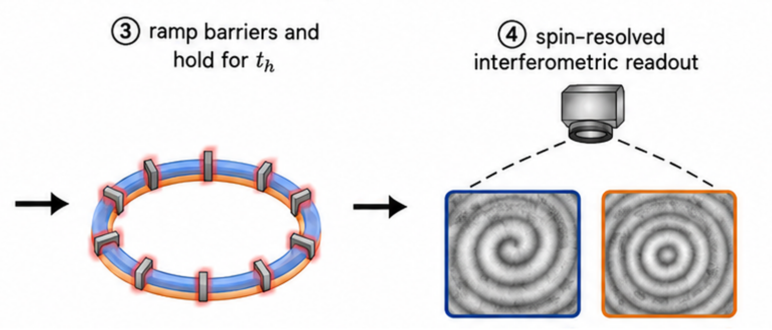

Through the entrainment coupling ρ_{12} it is dragged by condensate 1 and acquires a time-dependent Josephson current given by

$$\hat{n} \cdot \boldsymbol{j}_2^*(t) = -\frac{\hbar}{m_1\zeta_1}\frac{\rho_{12}}{\rho_{11}}|\Psi_{k=1,1}||\Psi_{k=2,1}|\sin[\Delta\theta_1 + \phi(t)]\,. \tag{38}$$

Oscillating at the *same* frequency ω_1 as the active condensate.

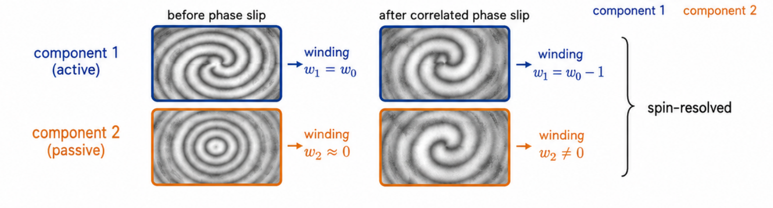

Through spin-resolved interferometry observe entrainment-induced current in the passive component osicllating at the Josephson frequency. In the limit $\rho_{12} \to 0$ (tuning the Feshbach resonance) this signal vanishes, providing a direct, in-situ measure of the entrainment coupling.

Possible other signatures

Theory shows that:

– the critical current is reduced by $\kappa_{12} = (\rho_{11} - \rho_{12})/\rho_{11}$ relative to the single-component value. Measuring the stability phase diagram (Pezze et al., Fig. 4) as a function of the Feshbach field, which tunes g_{12} and hence ρ_{12}, should reveal a downward shift of the critical line $w_c(n)$ as entrainment is switched on.

– Phase-difference control via chemical-potential mismatch $\mu_1 \neq \mu_2$. This sets $\Delta\theta_2 \neq 0$ across each junction and thereby directly controls the entrainment-mediated current of condensate 2.

Thank you for your attention